ARCHIWUM HYDROTECHNIKI
Tom XXXIX 1992 Zeszyt 1

*LESZEK M. KACZMAREK, RAFAŁ OSTROWSKI**

Modelling of wave-current boundary layers with application to surf zone

Notation

a_{1m} – free stream water particle motion amplitude;
d_{tr} – distance between sea bottom and wave trough;
g – acceleration of gravity;
h – mean water depth;
k_s – Nikuradse's roughness parameter;
k_w – bed apparent roughness;
p – pressure;
p_c – steady pressure;
p_w – unsteady pressure;
t – time;
T – wave period;
u – instantaneous velocity;
u_c – current velocity;
u_d – defect velocity;
u_f – friction velocity;
$\hat{u}_f$ – maximum friction velocity;

*Dr eng. L.M. KACZMAREK, Eng. R. OSTROWSKI – Institute of Hydroengineering, Polish Academy of Sciences, ul. Kościerska 7, 80-953 Gdańsk.

u_{fo} – current friction velocity;

u_{fc} – root mean square friction velocity;

u_w – horizontal oscillatory velocity;

$\overline{u_w^2}$ – mean square horizontal oscillatory velocity;

U – mean current velocity in outer region;

U_0 – free stream velocity;

U_{1m} – maximum free stream velocity;

U_m – total mean velocity;

V – slip velocity;

V_c – calculated total mean current velocity;

V_d – total mean current velocity of input data:

x – horizontal coordinate;

z – vertical coordinate:

z_0 – theoretical bed level;

$z_{\max}$ – validity limit of boundary layer motion equation;

δ – boundary layer thickness;

δ_1 – boundary layer thickness at moment corresponding to maximum free stream velocity;

ξ_{tr} – ordinate of wave trough;

$\bar{\eta}$ – set-up of water level;

κ – von Karman's constant;

ν_t – eddy viscosity;

ν_{tc} – eddy viscosity in outer undertow region;

ρ – water density;

τ – shear stress;

τ_0 – bottom shear stress;

τ_c – shear stress averaged over time;

τ_e – shear stress at lower limit of undertow outer region;

ω – angular frequency.

1. Introduction

The waves and currents interaction as a result of very specific unsteady flow is of interest of coastal engineering researchers for it governs sediment motion and the variability of bottom profile. The forces controlling and affecting sediment transport play key role close to the sea bed. Thus precise and possibly simple mathematical

description of the bottom boundary layer of wave and current origin is needed to solve the tasks mentioned above.

Taking into consideration the way turbulent wave – current boundary layer is generated one may distinguish two main cases dependent upon conditions and circumstances of wave and current interaction:

I – in which the presence of waves results in a boundary layer flow for current reflecting a much larger roughness parameter than would be expected on the basis of the physical bottom roughness; in other words flow turbulence is created by bottom friction in response to oscillatory motion of water nearby sea bed;

II – in which turbulence generated not by the flow near the bottom but rather by the breaking of the wave is quickly spreaded downwards from the free surface.

The case I mostly takes place in tidal regions and in estuaries. A three-layer time invariant eddy viscosity model employed to find an analytical solution has been given in Myrhaug and Slaattelid (1989; 1990). Some experimental results and comparisons with the theoretical ones are also shown. Laboratory experiment was made by van Doorn (1981) for two velocities of currents superposed on waves. The measurements used to be taken at a presence of wave turbulence maintained due to influence of artificial bottom roughness elements.

The case II concerns the phenomenon of the mass flux carried shoreward by the breaking waves. It is compensated by a seaward return flow or undertow. The recent approaches, published in Svendsen (1984) and Stive and Wind (1986) base on the solution of momentum equation at the presence of the roller and its effect on both the radiation stress and energy flux. The influence of the bottom boundary layer is neglected.

The aim of the present approach is to give better description of the mechanisms ruling two cases with taking into account the compatibility of the shear layer between the one at the upper limit of the bottom boundary layer bound with sea bed phenomena and the other one generated by the steady current. For this purpose iteration methods are involved to determine time-variable bottom shear stress and velocity distributions in both boundary layer and outer region.

The numerical solution of the equation of motion in wave and current boundary layer with the use of implicit method involving Crank–Nicholson scheme is proposed. The two–layer eddy viscosity model within the wave–current boundary layer is used. The primary difference between the present approach and the other ones is the use of solution of integral equation proposed by Fredsoe (1984) for evaluating of basic eddy viscosity characteristics. The numerical results are compared with experimental data in order to verify the validity of the model.

2. Wave and current boundary layer

2.1. Formulation of the problem

The turbulent bottom boundary layer is strongly affected by the sea bed roughness. The motion of the fluid is governed by the Navier-Stokes equation, the equation of

continuity and boundary conditions. The combined turbulent oscillatory and steady flow near the rough sea bottom is considered. For this case the motion equation, after neglection of the convective term, has the form:

$$\frac{\partial u}{\partial t} = -\frac{1}{\rho}\frac{\partial p}{\partial x} + \frac{\partial}{\partial z}\left(\frac{\tau}{\rho}\right) \tag{1}$$

where the total shear stress is identified as

$$\tau = \rho \nu_t \frac{\partial u}{\partial z} \tag{2}$$

Here ρ denotes the density of the fluid, t the time, z the ordinate normal to the bottom, ν_t the turbulent viscosity, p is the pressure consisting of the steady pressure p_c and the unsteady pressure p_w,

$$p = p_c + p_w \tag{3}$$

u is the velocity parallel to the bottom, i.e.

$$u(z,t) = u_c(z) + u_w(z,t) \tag{4}$$

where u_c is the current velocity and u_w the horizontal wave velocity. The equation of continuity is also satisfied since the velocity is a function of z only, i.e. independent of x.

The present analysis is taken to be valid for current velocities with an order of magnitude not exceeding that of the wave induced velocity. Thus, the present analysis treats the interaction of waves and currents in a wave-dominated environment. The shear stress is assumed to act only in the vicinity of boundaries limiting the oscillatory flow of the real liquid. At the upper limit of boundary layer the oscillatory flow may be described with the equation of motion for non-viscous liquid:

$$\frac{\partial U_0}{\partial t} = -\frac{1}{\rho}\frac{\partial p_w}{\partial x} \tag{5}$$

where U_0 is the free stream wave velocity parallel to the bottom outside the wave boundary layer. The term $\partial U_0/\partial t$ represents the horizontal pressure gradient since the vertical velocities are negligible very close to the sea bed.

Integrating Eq. (1) over the wave period

$$\int_0^T \frac{\partial u}{\partial t} dt = -\frac{1}{\rho}\frac{\partial}{\partial t}\int_0^T p\, dt + \frac{1}{\rho}\frac{\partial}{\partial t}\int_0^T \tau\, dt$$

and taking into account that

$$\int_0^T \frac{\partial u}{\partial t} dt = u|_0^T = 0$$

and: $\tau = \tau_c + \tau_w$
one obtains:

$$\frac{\partial \tau_c}{\partial z} = \frac{\partial p_c}{\partial x} \tag{6}$$

where

$$\tau_c = \frac{1}{T}\int_0^T \tau \, dt; \qquad p_c = \frac{1}{T}\int_0^T p \, dt \tag{7}$$

Because the shear stress is identified as in Eq. (2) and the velocity is the sum (4), time-averaged shear stress yields:

$$\tau_c = \rho \nu_t \frac{\partial u_c}{\partial z} \tag{8}$$

Here it is assumed that ν_t is time – independent. By subtracting Eq. (6) from Eq. (1), the governing equation for the wave motion is obtained as:

$$\frac{\partial u_w}{\partial t} = -\frac{1}{\rho}\frac{\partial p_w}{\partial x} + \frac{\partial}{\partial z}\left(\frac{\tau - \tau_c}{\rho}\right) = \frac{\partial U_0}{\partial t} + \frac{\partial}{\partial z}\left(\nu_t \frac{\partial u_w}{\partial z}\right) \tag{9}$$

Notice that the assumption of time – independence of eddy viscosity is very strong as it allows us to treat the combined current and wave motion by separate equations, i.e. Eqs (8) and (6) and Eq. (9) respectively. Also, the boundary conditions can be separated into boundary conditions for the current and wave motion, respectively.

Although the current motion and wave motion can be described by separate equations, there is a coupling between waves and current in corporated in the eddy viscosity. This appears in the modelling of ν_t. In this way because of neglection of the convective term in Eq. (1) all second order effects (in particular the Eulerian mean velocity just outside the boundary layer) are also not taken into account.

Myrhaug and Slaattelid using a three-layer time invariant eddy viscosity model proposed the analytical solutions of mentioned above separate equations, but the coupling problem in their solution is incorporated by the definitions of the friction velocities or bottom friction coefficients f_{cw} and f_s which can be solved in rather complicated iteration scheme (1989) or by a rational approach (1990).

In the contrary to Myrhaug's and Slaattelid's approaches the authors propose numerical solution of the total equation (1) with the assumption of logarithmic current velocity profile which means that the region close to the bottom is a region where the shear stress is constant.

Hence the considered flow in boundary layer is governed by the simplified Eq. (1) in the form:

$$\frac{\partial u}{\partial t} = \frac{\partial U_0}{\partial t} + \frac{1}{\rho}\frac{\partial \tau}{\partial z} \tag{10}$$

where Eqs (4) and (2) are still valid and outside the boundary layer by equation:

$$\frac{\partial u_c}{\partial z} = \frac{u_{fc}^2}{\nu_t} \tag{11}$$

Introducing the variable called defect velocity as (Brevik 1981):

$$u_d(z,t) = u(z,t) - U_0(t) \tag{12}$$

one obtains the simplified form of Eq. (10):

$$\frac{\partial u_d}{\partial t} = \frac{1}{\rho}\frac{\partial \tau}{\partial z} \tag{13}$$

The shear stress on the right hand side term of Eq. (13) may be expressed accordingly to Boussinesq's concept as follows:

$$\tau(z,t) = \rho\nu_t \frac{\partial u(z,t)}{\partial z} = \rho\nu_t \frac{\partial u_d(z,t)}{\partial z} \tag{14}$$

The substitution of Eq. (14) into Eq. (13) with the assumption $\Delta t = \Delta wt$ yields the non-dimensional in time equation of motion:

$$\frac{\partial u_d(z,t)}{\partial(wt)} = F_1(z)\frac{\partial^2 u_d}{\partial z^2} + F_2(z)\frac{\partial u_d}{\partial z} \tag{15}$$

in which

$$\begin{aligned} F_1(z) &= \frac{\nu_t(z)}{w} \\ F_2(z) &= \frac{1}{w}\frac{\partial[\nu_t(z)]}{\partial z} \end{aligned} \tag{16}$$

where w is angular frequency.

The present eddy viscosity model is an extension of Kajiura's (1968) and Brevik's (1981) model, and here the following three-layer eddy viscosity model is proposed (see Fig. 1):

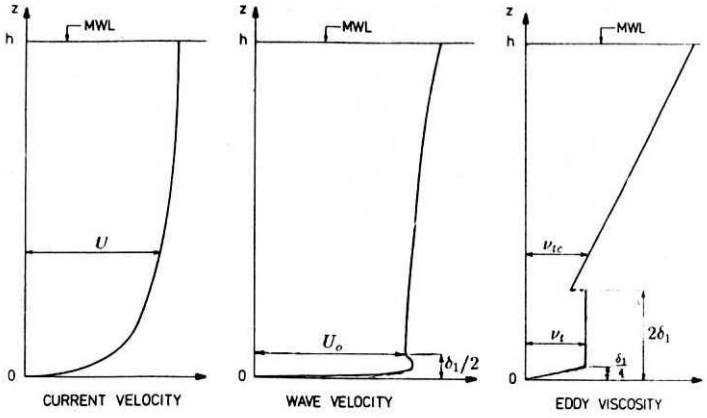

Fig. 1. Distributions of velocity and eddy viscosity

I – overlap layer

$$\nu_t(z) = \kappa \hat{u}_f z \quad \text{for } z_0 < z \leq \Delta \tag{17a}$$

II – outer layer

$$\nu_t = \kappa \hat{u}_f \Delta \quad \text{for } \Delta < z \leq z_{\max} \tag{17b}$$

III

$$\nu_t = \kappa u_{fc} z \quad \text{for } z > z_{\max} \tag{17c}$$

where $z_0 = k_s/30$, $\kappa = 0.4$ (von Karman's constant), $\hat{u}_f = \max[u_f(wt)]$, $\Delta = \delta/2$, δ is the thickness of boundary layer at the moment corresponding to maximum oscillatory velocity, k_s is Nikuradse's roughness parameter and $u_f(wt)$ is the friction velocity.

The quantities $\hat{u}_f, \delta$ are recommended to be determined from the solution of integral equation proposed by Fredsoe (1981, 1984), carried out in sections 2.2 and 2.3.

Eq. (17c) is certainly not valid near the free surface, where the turbulence is also damped, but this effect is neglected as the attention is focused on the bottom boundary layer problem.

The authors believe that such an approach is a reasonable compromise between accuracy and simplicity and this is its main benefit over Myrhaug's model.

2.2. Wave turbulent boundary layer approach

Eq. (10) is given, after integration, in the form:

$$-\frac{\tau_0}{\rho} = -u_f^2 = -\int_{k_s/30}^{\delta + k_s/30} \frac{\partial}{\partial t}(U_0 - u)dz \tag{18}$$

The boundary condition at the upper limit of the boundary layer reads:

$$\begin{aligned} z &= \delta + \frac{k_s}{30} \\ U_0 &= u \end{aligned} \tag{19}$$

or, accordingly to Jonsson's (1966) adaptation of the logarithmic velocity profile,

$$\frac{u}{u_f} = \frac{1}{\kappa} \ln \frac{30z}{k_s} \tag{20}$$

it converts to the formula:

$$\delta = \frac{k_s}{30}(e^{z_1} - 1) \tag{21}$$

in which

$$z_1 = \frac{U_0 \kappa}{u_f} \tag{22}$$

Eq. (18) is rearranged to the form:

$$-u_f^2 = -\delta\frac{dU_0}{dt} + \frac{1}{\kappa}\frac{du_f}{dt}\frac{k_s}{30}\left[e^{z_1}(z_1-1)+1\right] \tag{23}$$

The above relationship may be expressed with the use of derivative of Eq. (22)

$$\frac{dz_1}{dt} = \frac{z_1}{U_0}\frac{dU_0}{dt} - \frac{z_1}{u_f}\frac{du_f}{dt} \tag{24}$$

by the differential equation with variable z_1:

$$\frac{dz_1}{d(\omega t)} = \beta\frac{\sin(\omega t)}{e^{z_1}(z_1-1)+1} - \frac{z_1(e^{z_1}-z_1-1)}{e^{z_1}(z_1-1)+1}\frac{1}{U_0}\frac{dU_0}{d(\omega t)} \tag{25}$$

in which

$$\beta = \frac{30\kappa^2}{k_s}\frac{U_{1m}}{\omega} = 30\kappa^2\frac{a_{1m}}{k_s} \tag{26}$$

where U_{1m} denotes maximum oscillatory velocity and a_{1m} the amplitude of water particle motion at the upper limit of the boundary layer.

The numerical solution of Eq. (25) yields time – dependent distributions of friction velocity $u_f(\omega t)$ and thickness of the boundary layer $\delta(\omega t)$, cf. Fig. 3.

2.3. Wave and current boundary layer approach

When the current is superposed on waves, Eq. (10) has, after integration, the form:

$$\frac{\tau(\delta)}{\rho} - \frac{\tau_0}{\rho} = -\int_{k_s/30}^{\delta+\frac{k_s}{30}}\frac{\partial}{\partial t}(U_0-u)\,dz \tag{27}$$

where

$$\tau(\delta) = \rho\, u_{f0}^2 \tag{28}$$

is the shear stress at the upper limit of the boundary layer and

$$\tau_0 = \rho|u_f|u_f \tag{29}$$

is the bottom shear stress, u_{f0} is the friction velocity of current origin ($at\ z=\delta$).

After making some assumptions and conducting transformations analogical as in the section 2.2 one obtains Eq. (27) in the form:

$$\frac{dz_1}{d(\omega t)} = \frac{30z_1^2\left[\left|\frac{\kappa U_0}{z_1}+u_{f0}\right|\left(\frac{\kappa U_0}{z_1}+u_{f0}\right)-u_{f0}^2\right]}{\omega k_s U_0\left[e^{z_1}(z_1-1)+1\right]} - \frac{z_1(e^{z_1}-z_1-1)}{e^{z_1}(z_1-1)+1}\times$$
$$\times\frac{1}{U_0}\frac{dU_0}{d(\omega t)} \tag{30}$$

in which

$$z_1(\omega t) = \frac{\kappa\, U_0}{u_f - u_{f0}} \tag{31}$$

The time – distributions of $u_f(\omega t)$ and $\delta(\omega t)$ are given in Fig. 7, for example.

It was proved that the distributions of friction velocity and boundary layer thickness are strongly affected by water particle motion amplitude to bottom roughness ratio and also by the current velocity – cf. Fredsoe (1984) for detailed discussion.

The current Friction velocity u_{f0}, besides the variable z_1, is unknown. Therefore the use of iteration method is proposed.

2.4. Solution of the problem

Equation (15) is solved numerically with the use of an implicit method involving Crank – Nicholson scheme for both wave motion and wave – current one.

The following boundary conditions are assumed:

$$u_d\left(z, \frac{\pi}{2}\right) = -V \quad \text{(approximate initial condition)} \tag{32}$$

$$u_d(0, \omega t) = -U_{1m} \cos(\omega t) - V \tag{33}$$

$$u_d(z_{\max}, \omega t) = 0 \tag{34}$$

where V denotes the steady current velocity at the height $z = z_{\max}$ ($V = 0$ for pure oscillatory motion).

Eqs. (15) and (11) are solved in boundary layer and outer region, respectively. The continuity of velocity profiles at $z = z_{\max}$ is satisfied. The limit $z_{\max}$ was estimated as $z_{\max} \simeq 2\delta_1$ (Kaczmarek, Ostrowski 1989); δ_1 is the value $\delta(t)$ calculated on the basis of equations (25) and (30) at the moment corresponding to maximum oscillatory velocity.

For pure wave motion the computations for the conditions of Jonsson's and Carlsen's (1976) experiment were performed. The comparison of measured and computed velocity profiles is shown in Fig. 2. Time distributions of the thickness of boundary layer δ the

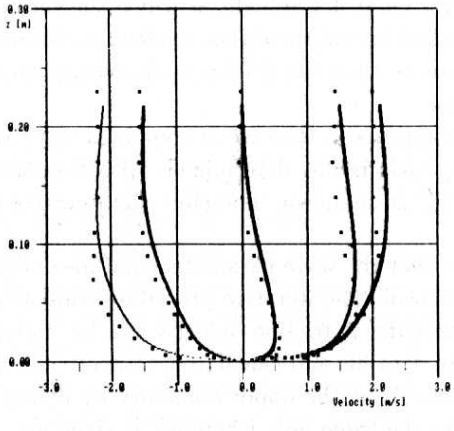

Fig. 2. Measured and prediced velocity profiles for test No 1 (Jonsson and Carlsen, 1976)

friction velocity u_f, both the one calculated on the basis of Eq. (25) and the other one determined from the equation:

$$u_f = \sqrt{\frac{\tau(z_0, \omega t)}{\rho}} \tag{35}$$

in which τ is estimated with the use of Eq. (14), are shown in Fig. 3.

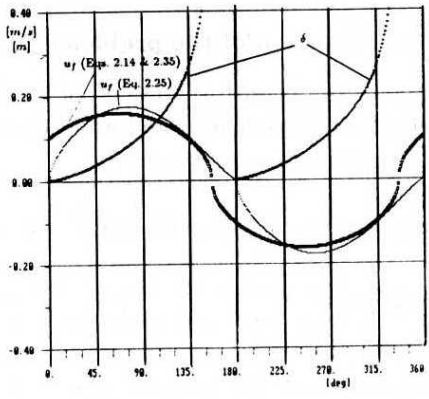

Fig. 3. Friction velocity and boundary layer thickness for test No 1 (Jonsson and Carlsen, 1976)

The accuracy of determination of velocity profiles seems to be good enough and also distributions of u_f calculated from Eq. (15) and Eq. (35) show the compatibility of maximum values. The advantage of the one given with Eq. (35) is that it has a phase shift in respect to free steam velocity. The analysis of boundary layer thickness distribution and its comparison with the maximum boundary layer thickness resulting from Fig. 2 leads to the conclusion that the one determined from Eq. (25) at the moment corresponding to maximum oscillatory velocity expresses rather the thickness of the friction boundary layer i.e. it is the hight at which the shear stress decreases to zero. Thus the well – known fact is confirmed that the friction boundary layer thickness δ_1 reaches twice higher ordinate than the thickness of velocity boundary layer δ (the one of traditional approach).

More sophisticated task appears in the case of combined wave and current motion, for the quantity u_{f0} in Eq. (30) is not determined. Also the value V in the boundary conditions (32) and (33) is unknown. Therefore the iterative procedure must be involved.

The assumption is made that the wave parameters and mean current velocity (averaged over the depth) are known. The iterative procedure consists of two main loops: external – searching for the current friction velocity u_{f0} by matching mean current velocities V_d and V_c, given in data file and calculated, respectively; internal – searching fro the steady current velocity V at the upper boundary by fitting the time averaged shear stress from Eq. (14) to the value ρu_{fc}^2 where u_{fc}^2 is given as:

$$u_{fc}^2 = \overline{u_f^2(\omega t)} \tag{36}$$

The concise scheme of the iteration method is given in Fig. 4.

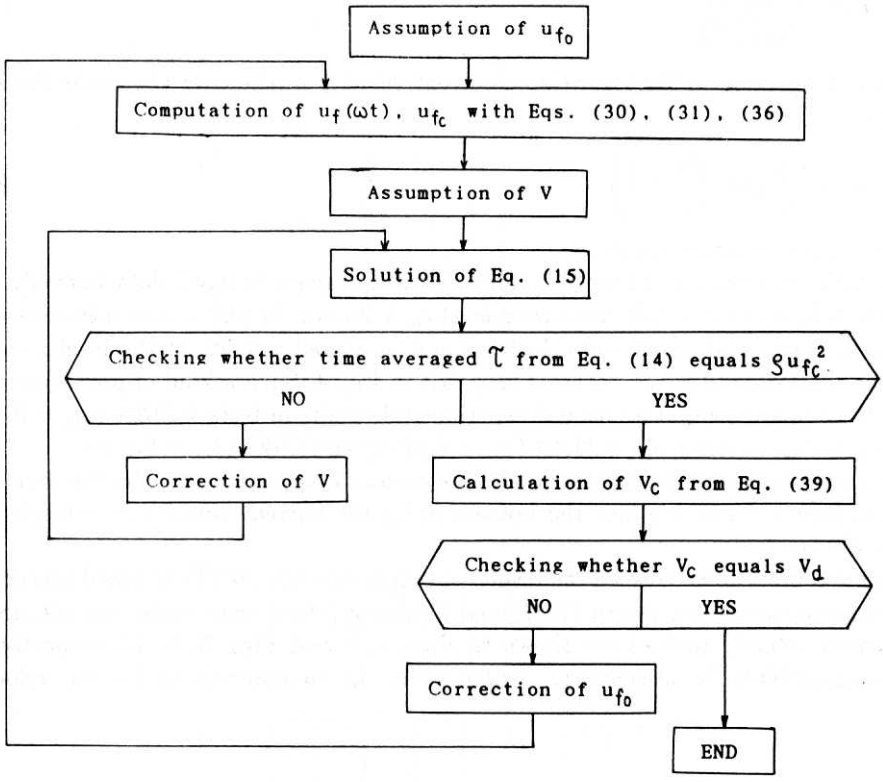

Fig. 4. Scheme of the iteration procedure for case I

Mean current velocity at the upper limit of validity of Eq. (15) with the assumption of logarythmic velocity profile reads:

$$V = \frac{u_{fc}}{\kappa} \ln \frac{30 z_{\max}}{k_w} \tag{37}$$

where k_w is the apparent roughness parameter.

This apparent roughness reflects the influence of the waves on the current, and is introduced in Eq. (37) in analogous form to the roughness used for steady, unidirectional rough, fully turbulent flow. For coupled motion of waves and current the presence of waves results in a larger resistance felt by the current outside the wave boundary layer, than when no waves are present. This increased resistance manifests itself as an apparent roughness larger than the physical roughness. Thus the presence of waves results in a reduction in the current velocities compared to the situation when no waves are present.

From Eq. (37) one obtains the formula for k_w:

$$k_w = \frac{30 z_{\max}}{\exp\left(\frac{V \cdot \kappa}{u_{fc}}\right)} \tag{38}$$

The integration of the logarithmic current velocity profile over the water depth h yields:

$$V_c = \frac{u_{fc}}{\kappa}\left(\ln \frac{30h}{k_w} - 1\right) \tag{39}$$

where h denotes water depth.

Sometimes total mean current velocity V_d is not given in input data but only the current velocity at a certain measuring level z_m is known. In such a case it is necessary to check the coincidence of the calculated and measured velocity at the level $x = z_m$, not the total quantities, cf. external loop exit in Fig. 4. Such a kind of procedure was used to compare computations and experimental results in tests $V10RA$ ($z_m = 0.1$ m and $z_m = z_{\max} = 0.016$ m), $V20RA$ ($z_m = 0.07$ m) and $CW1$ ($z_m = 0.8$ m).

Thus in the formulation of the model the current is specified either by the averaged current over a depth h above the bottom or by the current velocity at a height z_m above the sea bed.

Some comparisons between the results obtained with the use of presented procedure and experiments of van Doorn (1981) and Myrhaug (1989) were made. Instantaneous and mean velocity profiles are shown in Figs. 6, 9 and Figs. 5, 8, 11, respectively. The compatibility is satisfactory. Additionally the comparisons of friction velocity

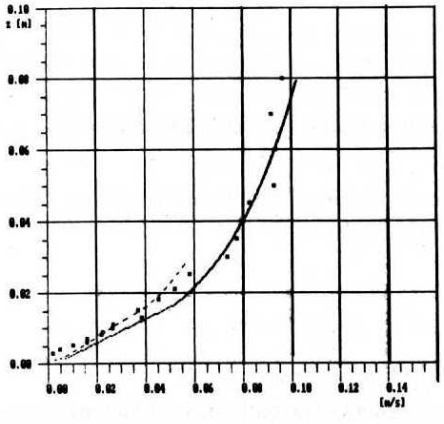

Fig. 5. Measured and predicted mean velocity profile for test $V10RA$ (van Doorn, 1981): – velocity matched at $z = 0.1$ m; - - velocity matched at $z = z_{\max}$

computed by Fredsoe's formula (Eq. 30) and numerically (Eqs. 14 and 35) are shown in Figs. 7, 10, 11. The present model obtains equal maximum values of u_f calculated in two ways. Some incompatibilities occur in other time periods as Fredsoe's method is an approximate one, based on the idea that the unsteady flow can be regarded as

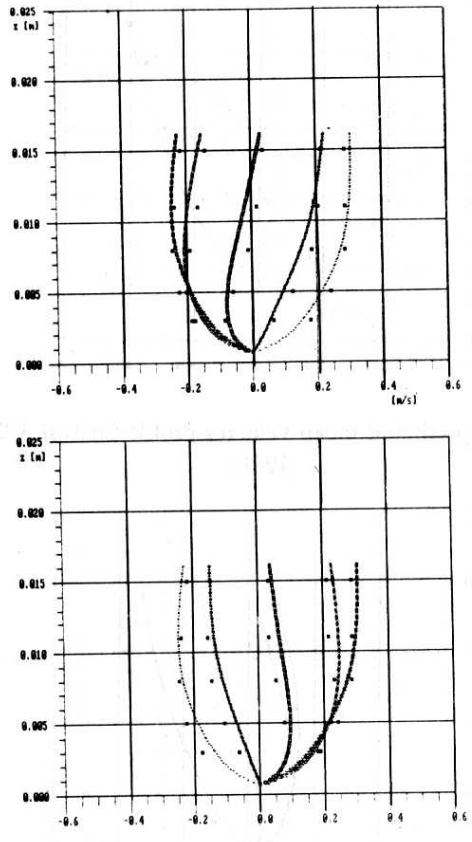

Fig. 6. Measured and predicted instantaneous velocity profiles in boundary layer for test $V10RA$ (van Doorn, 1981)

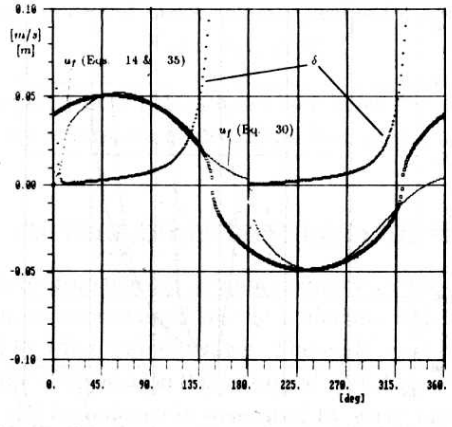

Fig. 7. Friction velocity and boundary layer thickness for test $V10RA$ (van Doorn, 1981)

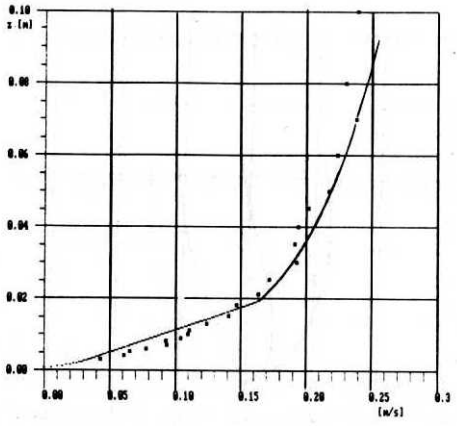

Fig. 8. Measured and predicted mean velocity profile for test $V20RA$ (van Doorn, 1981)

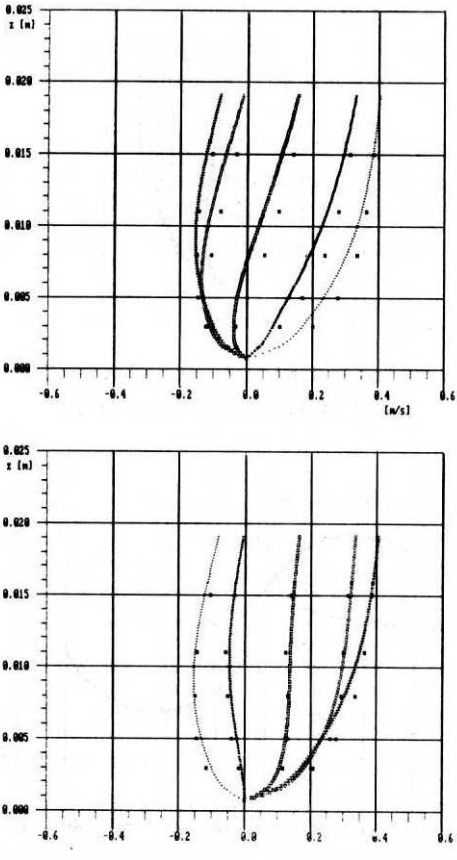

Fig. 9. Measured and predicted instantaneous velocity profiles in boundary layer for test $V20RA$ (van Doorn, 1981)

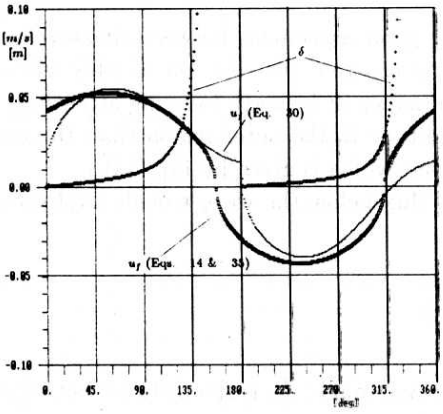

Fig. 10. Friction velocity and boundary layer thickness for test *V20RA* (van Doorn, 1981)

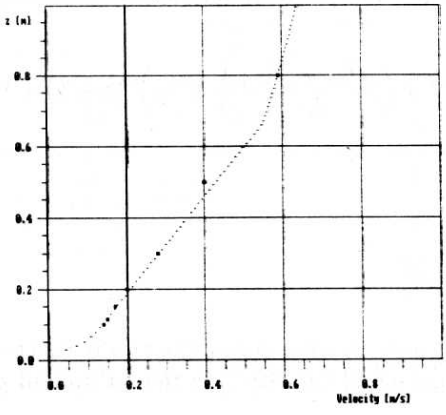

Fig. 11. Measured and predicted mean velocity profile for test *CW*1 (Myrhaug and Slaattelid, 1989)

a growing boundary layer, where a new boundary layer develops every time the flow reverses, i.e. the memory effects are neglected as long as the boundary layer thickness is small.

3. Wave – current boundary layer in the surf zone

The case of the wave propagating perpendicularly to the shoreline is considered. The oscillatory motion is accompanied by the undertow which compensates the mass flux carried shoreward by the breaking waves. The eddy viscosity model in the bottom boundary layer the same as in section 2 is assumed – cf. Eqs. (17a, b). Considering the outer region in which the turbulence is generated by wave breaking one should admit that the vertical distribution of the eddy viscosity is not fully recognized yet. Svendsen (1984) takes two kinds of distribution of ν_t constant and exponential into account

and finds out reasonably good agreement between measurements and predictions of velocity profiles. Thus the constant distribution of eddy viscosity in outer region is assumed in the presented paper. It is worth focusing attention on the fact that ν_t is of much greater order magnitude in the outer region than the one in the upper part of the bottom boundary layer, which is given by Eq. (17b).

The total mean mass flux below the wave trough level should balance that above this level, implying that:

$$U_m \, d_{tr} = \int_{-h}^{\xi_{tr}} U(z) \, dz \tag{40}$$

where ξ_{tr} is the level of wave trough, d_{tr} is the distance betweem sea bottom and wave trough.

The variable $U(z)$ is the mean current velocity in the outer region, the coordinate system begins at mean water level and z axis is directed upwards. The vertical distribution of the quantity $U(z)$ may be estimated by the following formula, cf. Svendsen (1984):

$$U(z) = \frac{1}{2} \alpha (z+h)^2 + \left(2 \frac{U_m - V}{d_{tr}} - \frac{1}{3} \alpha \, d_{tr} \right) (z+h) + V \tag{41}$$

in which

$$\alpha = \alpha_1(x)/\nu_{tc} \tag{42}$$

$$\alpha_1(x) = \frac{\partial}{\partial x} \left(\overline{u_w^2} + g\bar{\eta} \right) \tag{43}$$

where ν_{tc} is the eddy viscosity in outer region (vertically constant), $\overline{u_w^2}$ is mean square oscillatory part of the horizontal velocity, $\bar{\eta}$ is the set-up and g is the acceleration of gravity.

The derivative of the relationship (41) reads:

$$\frac{\partial U(z)}{\partial z} = \alpha \, (z+h) + \left(2 \frac{U_m - V}{d_{tr}} - \frac{1}{3} \alpha \, d_{tr} \right) \tag{44}$$

The shear stress at the lower limit of the undertow region is given by the formula:

$$\tau_e = \rho \nu_{tc} \left. \frac{\partial U(z)}{\partial z} \right|_{z=-h} \tag{45}$$

Basically, the slip velocity V, which corrensponds to the one at the validity limit of boundary layer motion equation (15) determined in section 2, is unknown and that is the reason for involving the iterative procedure in the solution of the problem.

As a little different phenomenon is considered, the iteration scheme used in the previous section of the paper (Fig. 4) has to be rearranged. In this case the quantity ν_{tc} should be given explicitly to evaluate the shear stress in the outer region to be matched with the friction at the upper limit of bottom boundary layer.

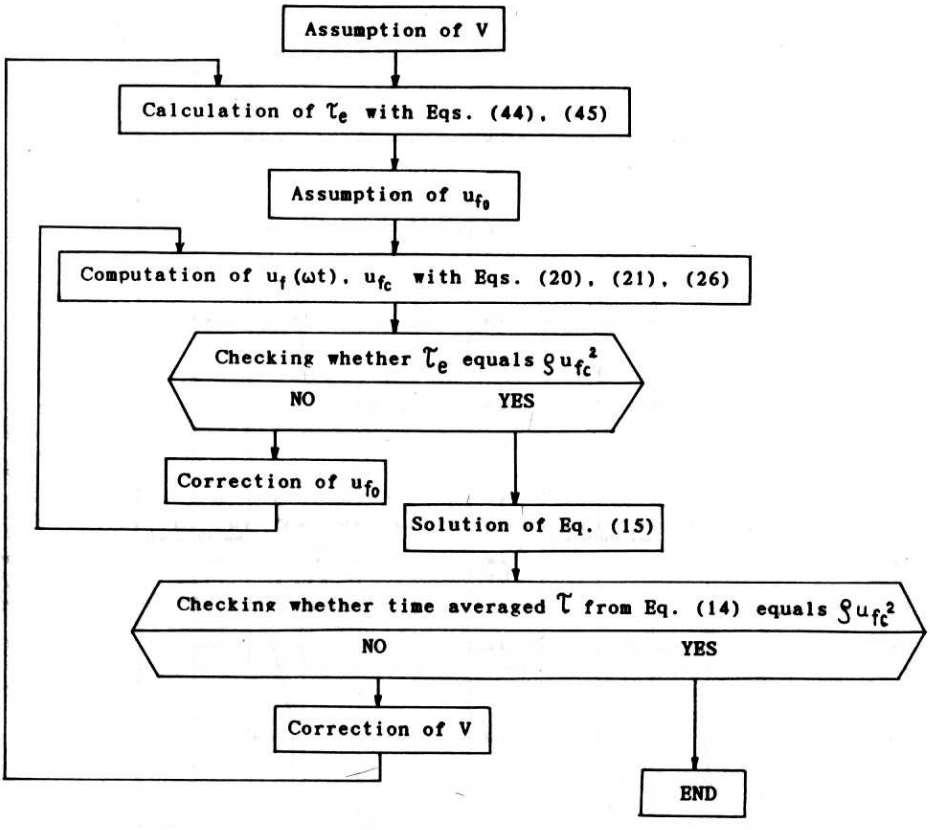

Fig. 12. Scheme of the iteration procedure for case II

The condensed scheme of the iteration method is shown in Fig. (12).

The comparisons between the measurements of Stive and Wind and Buhr – Hansen and Svendsen experiments (Stive and Wind 1986) and the results obtained with the use of proposed method are shown in Figs. (14) and (15).

Computed instantaneous velocity profiles are given in Fig. (15) as an example. Experiments parameters are given in Tab. 1.

As it is seen the slip velocity obtained with the use of presented procedure does not differ much from that which would exist if an assumption were made of $\tau_e(z = -h)$ equal zero. This confirms experimental observations of Stive and Wind (1986). The above conclusion is of a great importance for calculating the undertow velocity distribution in practical use. Thus the present method for computation the slip velocity simplifies considerably using Eq. (44)

$$\left.\frac{\partial U(z)}{\partial z}\right|_{z=-h} = 0 \tag{46}$$

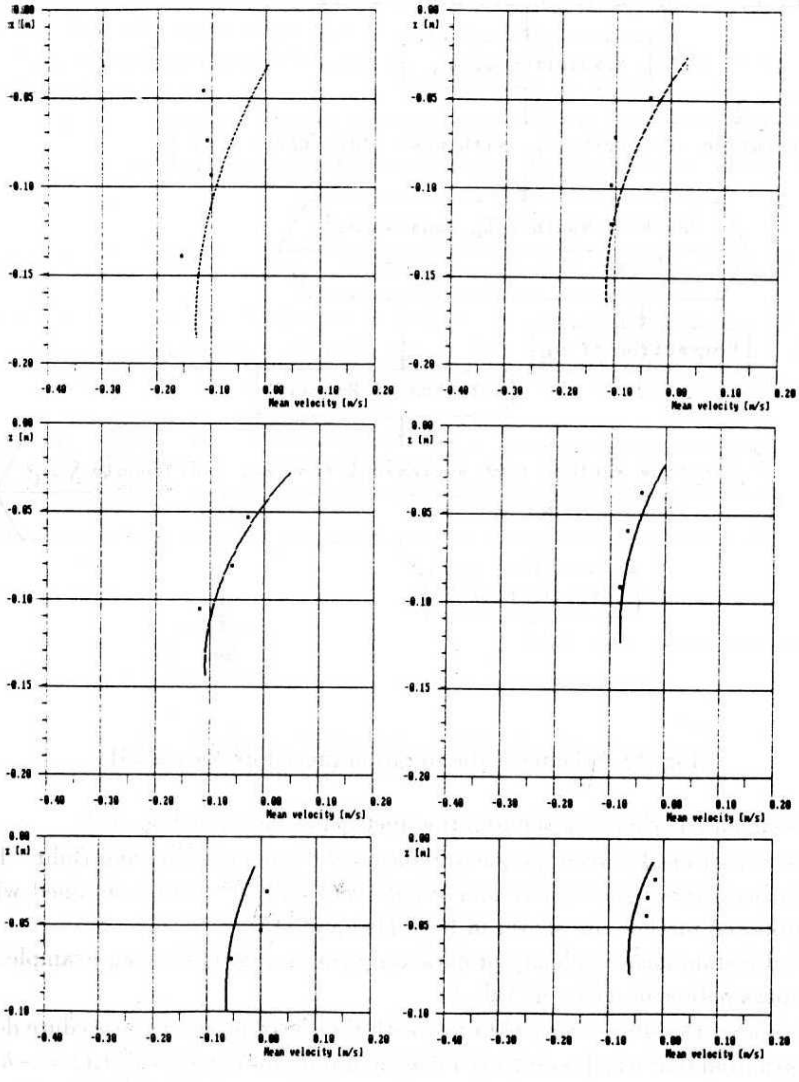

Fig. 13. Measured and predicted undertow for experiment of Stive and Wind (1986)

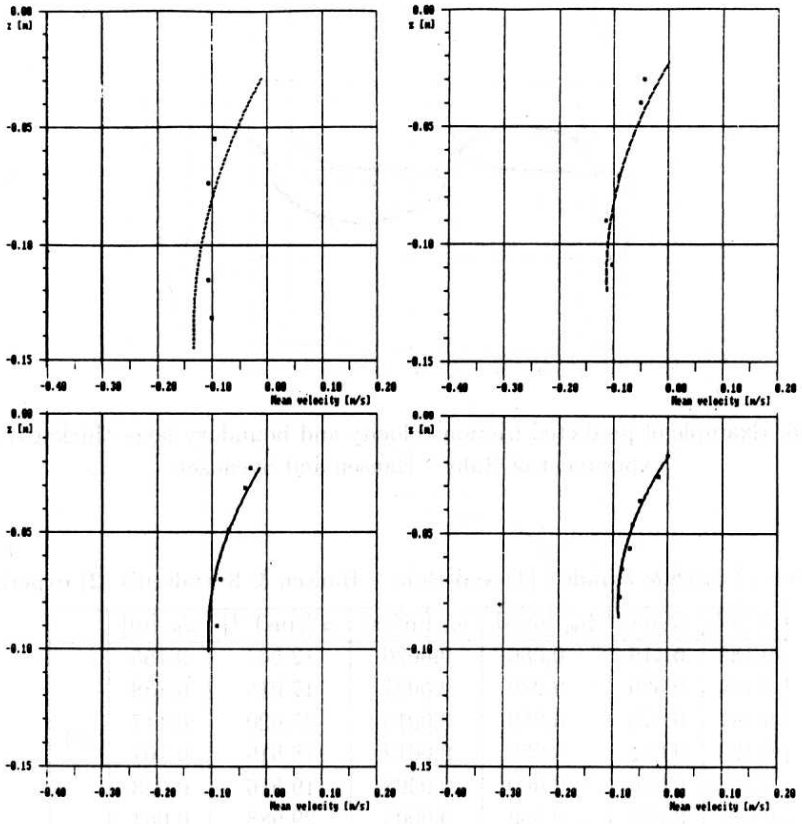

Fig. 14. Measured and predicted undertow for experiment of Buhr – Hansen and Svendsen (Svendsen, 1984)

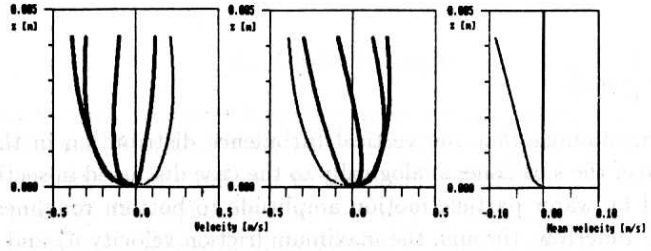

Fig. 15. Example of predicted instantaneous and mean velocity profiles in boundary layer for experiment of Buhr – Hansen and Svendsen

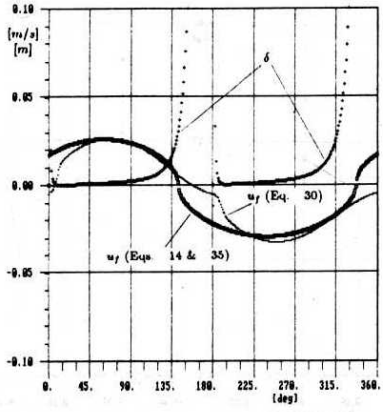

Fig. 16. Example of predicted friction velocity and boundary layer thickness for experiment of Buhr – Hansen and Svendsen

Table 1

Parameters of Stive & Winds's (1) and Buhr – Hansen & Svendsen's (2) experiment

h [m]	H [m]	U_m [m/s]	ν_{tc} [m^2/s]	α [(ms)$^{-1}$]	d_{tr} [m]	
0.185	0.119	– 0.086	0.0026	12.565	0.155	
0.164	0.090	– 0.070	0.0021	17.015	0.138	
0.144	0.070	– 0.059	0.0016	25.620	0.117	(1)
0.123	0.061	– 0.057	0.0012	18.519	0.101	
0.100	0.046	– 0.049	0.0008	19.516	0.083	
0.077	0.035	– 0.050	0.0005	29.988	0.064	
0.145	0.116	– 0.095	0.0017	21.185	0.117	
0.120	0.087	– 0.078	0.0013	28.271	0.097	(2)
0.101	0.072	– 0.071	0.0000	36.325	0.078	
0.086	0.058	– 0.062	0.0008	46.419	0.069	

to the formula:

$$V = U_m - \frac{1}{6}\,\alpha\, d_{tr}^2 \tag{47}$$

It is worth mentioning that the vertical turbulence distribution in the boundary layer for the case of the surf zone, analogically to the case discussed in section 2, is also strongly affected by water particle motion amplitude to bottom roughness ratio and mean velocity of undertow, through the maximum friction velocity $\hat{u_f}$ and the value of δ_1.

In the computations k_s was assumed as 1 mm for all sets of data after Svendsen and Buhr – Hansen (1988). Additionally the computations were performed for one set of data with $k_s = 0.5$ cm, for checking the influence of the roughness parameter. The results for the case in which $k_s = 0.5$ cm are given in Fig. 17. The conclusion has been

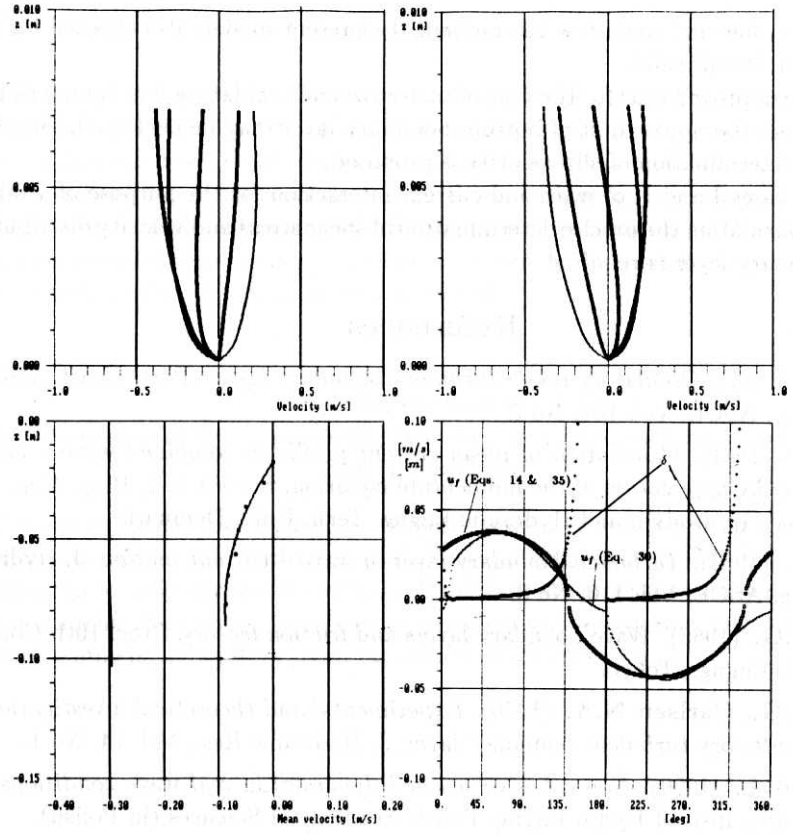

Fig. 17. Example of predicted velocity profiles, friction velocity and boundary layer thickness in experiment of Buhr – Hansen and Svendsen for $k_s = 5$ mm

made that the roughness parameter value does not affect the mean undertow profile very much but bottom shear stress and velocity profiles in the boundary layer strongly depend on it.

4. Conclusions

In this paper wave – current boundary layer concept is presented. In the model Kajiura's (1968) and Brevik's (1981) eddy viscosity models have been adapted. The iteration method has been employed to determine shear stress distributions in time and velocity profiles. The equation of motion in the boundary layer is solved numerically. Comparisons are made with some laboratory experiments and a good agreement between experimental results and predictions is reached. Two types of combined wave and current boundary layers have been discussed.

The concept of boundary layer has been involved in two kinds of wave and current interaction. For the case when the turbulence in outer region (in which logarithmic velocity distribution exists) is generated by the flow near the bottom and for the case

of oscillatory flow and undertow interaction, the present model, also checked for pure wave motion, is still valid.

It has been proved that for the case of undertow and oscillatory flow interaction the shear stress at the upper limit of bottom boundary layer may be neglected. Simplified method of determination of slip velocity is proposed.

In both cases I and II of wave and current interaction for the purpose of sediment transport calculation the precise determination of shear stress and velocity distributions in the boundary layer is required.

References

Brevik I. (1981), *Oscillatory rough turbulent boundary layers,* Port. Coast., and Oc. Engng., ASCE, Vol. 107, No 3.

Fredsoe J. (1981), *Calculation of mean current profile in combined wave – current motion by application of the momentum equation,* Parts 1 & 2, Prog. Rep. 55 & 56, Inst. Hydrodyn. and Hydraulic Engng. Tech. Univ. Denmark.

Fredsoe J. (1984), *Turbulent boundary layer in wave – current motion,* J. Hydraulic Engng, ASCE, Vol. 110, No 8.

Jonsson I.G. (1966), *Wave boundary layers and friction factors,* Proc. 10th Conf. on Coast. Engng., Tokyo.

Jonsson I.G., Carlsen N.A. (1976), *Experimental and theoretical investigations in an oscillatory turbulent boundary layer,* J. Hydraulic Res., Vol. 14, No 1.

Kaczmarek L. (1990), *Non-cohesive sea bed dynamics in real wave conditions,* Ph. D. thesis, Inst. of Hydro-Engng. Polish Academy of Sciences (in Polish).

Kaczmarek L., Ostrowski R. (1989), *The analysis of the bed friction and description of the shear stress transmission into the sea bed* (in Polish), Internal Rep. IBW PAN, Gdańsk.

Kajiura K. (1968), *A model of the bottom boundary layer in water waves,* Bull. Earthquake Res. Inst., Vol. 46, Tokyo.

Myrhaug D., Slaattelid O.H. (1989), *Combined wave and current boundary layer model for fixed rough seabeds,* Ocean Engng., Vol. 16, No. 2.

Myrhaug D., Slaattelid O.H. (1990), *A rational approach to wave – current friction coefficients for rough, smooth and transitional turbulent flow,* Coast. Engng., Vol. 14, 265-293.

Stive M.J.F., Wind H.G. (1986), *Cross – shore mean flow in the surf zone,* Coast. Engng., Vol. 10, 325-340.

Svendsen I.A. (1984), *Mass flux and undertow in a surf zone,* Coast. Engng., Vol. 8, 347-365.

Summary

In this paper wave–current boundary layer concept is presented. In the model Kajiura's (1968) and Brevik's (1981) eddy viscosity models have been adapted. The iteration method has been employed to determine shear stress distributions in time and velocity profiles. The equation of motion in the boundary layer is solved numerically. Comparisons are made with some laboratory experiments and a good agreement between experimental results and predictions is reached. Two types of combined wave and current boundary layers have been discussed.

Streszczenie

Modelowanie falowo – prądowej warstwy przyściennej zastosowane do strefy przyboju

W pracy przedstawiono koncepcję falowo – prądowej warstwy przyściennej wykorzystującą modele lepkości turbulentnej Kajiurya (1968) i Brevika (1981). Zastosowano iteracyjną metodę do określenia chwilowych rozkładów naprężeń stycznych i prędkości. Równanie ruchu dla warstwy przyściennej rozwiązano numerycznie. Otrzymano dobrą zgodność pomiędzy laboratoryjnymi pomiarami a obliczeniami.